Glycobiology vol. 15 no. 1 pp. 21–29, 2005
doi:10.1093/glycob/cwh135
Advance Access publication on August 11, 2004

TNFα-induced insulin resistance in adipocytes as a membrane microdomain disorder: involvement of ganglioside GM3

Kazuya Kabayama[2,3], Takashige Sato[2], Futoshi Kitamura[2], Satoshi Uemura[2], Byoung Won Kang[2], Yasuyuki Igarashi[2], and Jin-ichi Inokuchi[1,2,3]

[2]Department of Biomembrane and Biofunctional Chemistry, Graduate School of Pharmaceutical Sciences, Frontier Research Center for Post-Genomic Science and Technology, Hokkaido University, Kita 21-Nishi 11, Kita-ku, Sapporo 001-0021, Japan; and [3]Core Research for Evalutional Science and Technology Program (CREST), Japan Science and Technology Corporation (JST), Graduate School of Pharmaceutical Sciences, Frontier Research Center for Post-Genomic Science and Technology, Hokkaido University, Kita 21-Nishi 11, Kita-ku, Sapporo 001-0021, Japan

Received on May 26, 2004; revised on August 2, 2004; accepted on August 4, 2004

Membrane microdomains (lipid rafts) are now recognized as critical for proper compartmentalization of insulin signaling, but their role in the pathogenesis of insulin resistance has not been investigated. Detergent-resistant membrane microdomains (DRMs), isolated in the low-density fractions, are highly enriched in cholesterol, glycosphingolipids and various signaling molecules. Tumor necrosis factor alpha (TNFα) induces insulin resistance in type 2 diabetes, but its mechanism of action is not fully understood. In other studies we have found a selective increase in the acidic glycosphingolipid ganglioside GM3 in 3T3-L1 adipocytes treated with TNFα, suggesting a specific function for GM3. In the DRMs from TNFα-treated 3T3-L1 adipocytes, GM3 levels were doubled compared with results in normal adipocytes. Additionally, insulin receptor (IR) accumulations in the DRMs were diminished, whereas caveolin and flotillin levels were unchanged. Furthermore, insulin-dependent IR internalization and intracellular movement of the IR substrate 1(IRS-1) were both greatly suppressed in the treated cells, leading to an uncoupling of IR–IRS-1 signaling. GM3 depletion was able to counteract the TNFα-induced inhibitions of IR internalization and accumulation into DRMs. Together, these findings provide compelling evidence that in insulin resistance the insulin metabolic signaling defect can be attributed to a loss of IRs in the microdomains due to an accumulation of GM3.

Key words: detergent-resistant microdomain (DRM)/ganglioside GM3/insulin receptor/insulin resistance/lipid rafts

Introduction

Insulin has multiple, tissue-specific effects on cells, which are elicited through both metabolic and mitogenic signaling. In culture, insulin can act as a growth factor for cells, sharing many mitogenic signaling pathways with other growth factors. However, the metabolic effects of insulin are unique and cannot be reproduced with other cellular stimuli.

Insulin resistance, defined as the decreased ability of cells or tissues to respond to physiological levels of insulin, is thought to be the primary defect in the pathophysiology of type 2 diabetes (Virkamaki *et al.*, 1999). Numerous studies have implicated tumor necrosis factor alpha (TNFα) as having a role in insulin resistance, both in cultured adipocyte and whole-animal models (Hotamisligil *et al.*, 1993, 1995; Uysal *et al.*, 1997). In adipocytes cultured in relatively low concentrations of TNFα (which does not cause a generalized suppression of gene expression), interference with insulin action occurs. This effect requires prolonged treatment (at least 72 h), unlike many acute responses to this cytokine (Guo and Donner, 1996). This protracted effect suggests that TNFα induces the synthesis of an inhibitor that is the actual effector.

One clue as to the mechanism of this hormone's unique actions may lie in the compartmentalization of the signaling molecules themselves. Cellular membranes contain subdomains called detergent-resistant microdomains (DRMs), because they are detergent-insoluble and highly enriched in cholesterol and glycosphingolipids (GSLs), but lacking in phospholipids (Hakomori, 2000; Simons and Toomre, 2000). Within the past decade, data have emerged from many laboratories implicating these lipid microdomains as critical for proper compartmentalization of insulin signaling in adipocytes (reviewed in Bickel, 2002, and Cohen *et al.*, 2003).

Gangliosides, a family of sialic acid–containing GSLs, are an important component of DRMs. In adipose tissues from various species, including human and mouse, GM3 is the most abundant ganglioside (Ohashi, 1979). Recently, we reported that in mouse 3T3-L1 adipocytes insulin resistance induced by TNFα was accompanied by increased GM3 expression. Indeed, we demonstrated that a chronic state of insulin resistance in adipocytes, induced by 100 pM TNFα, was accompanied by an up-regulation of GM3 synthesis at the transcriptional level. Moreover, the pharmacological depletion of GM3 prevented a TNFα-induced defect in insulin-dependent tyrosine phosphorylation of insulin receptor substrate-1 (IRS-1), providing evidence that GM3 functions as an inhibitor of insulin metabolic signaling during chronic exposure to TNFα (Tagami *et al.*, 2002). We were able to extend these *in vitro* observations to living animals using obese Zucker *fa/fa* rats and *ob/ob* mice,

[1]To whom correspondence should be addressed; e-mail: inokuchi@kinou02.pharm.hokudai.ac.jp

in which the GM3 synthase mRNA levels in the white adipose tissues are significantly higher than in their lean controls (Tagami *et al*., 2002).

In the present study, we examine the effect of TNFα on the composition and function of DRMs in adipocytes and demonstrate that increased GM3 levels result in the elimination of insulin receptors (IRs) from the DRMs, whereas caveolin and flotillin remain in the DRMs. Thus we present a new pathological feature of insulin resistance in adipocytes induced by TNFα.

Results

GM3 but not ceramide is increased in adipocytes in a chronic state of insulin resistance

We reported previously that the state of insulin resistance in 3T3-L1 adipocytes induced by TNFα is accompanied by increased GM3 ganglioside expression through up-regulation of GM3 synthase (SAT-I) gene expression (Tagami *et al*., 2002). TNFα activates several signaling cascades, including the stimulation of sphingomyelinase and consequent ceramide production (Hannun, 1994). Exogenous sphingomyelinase and cell-permeable (short-chain) ceramides have been shown to mimic some effects of TNFα, including decreases in the insulin-dependent tyrosine phosphorylation of IRS-1 (Kanety *et al*., 1996; Peraldi *et al*., 1996) and glucose uptake (Brindley *et al*., 1999). Therefore we examined endogenous ceramide production in TNFα-treated adipocytes. After TNFα treatment, ceramide levels doubled throughout the first 6 h of treatment, then returned to control levels by 24 h (Figure 1A). At 96 h, though, there was no increase, suggesting that ceramide has no role in insulin signaling during the chronic state of TNFα-induced insulin resistance. Using the same lipid extracts, we observed a prolonged increase in GM3 levels as reported previously (Tagami *et al*., 2002). The increase in GM3 appeared as early as 1 h, reaching a plateau at 48 h, and remained at a high level throughout the chronic TNFα treatment (96 h) (Figure 1B). These findings led us to investigate the pathophysiological role(s) of GM3 in adipocytes having a state of insulin resistance.

IR is a component of the DRMs and is selectively eliminated from the DRMs during a state of insulin resistance induced by TNFα

Studies of the presence of IRs in DRMs/caveolae have provided conflicting data (Gustavsson *et al*., 1999; Kimura *et al*., 2002; Mastick and Saltiel, 1997; Muller *et al*., 2001). We evaluated the localization of IRs in a flotation assay following extraction with increasing concentrations of Triton X-100 or under hypertonic alkaline conditions (500 mM sodium carbonate) (Figure 2). In the carbonate buffer, IRs from normal 3T3-L1 cells were found exclusively in the low-density, insoluble fractions 4 and 5, which are known to carry DRMs, whereas a small portion of the IRs in TNFα-treated cells shifted to fractions 6–8. On the other hand, there was no accumulation in the DRMs in cells, untreated or treated with TNFα, when examined using an extraction buffer containing 1% (data not shown) or 0.1% Triton X-100, concurring with a previous report using high levels of detergent (Gustavsson *et al*., 1999). However, when the flotation assay was performed using buffer with lower concentrations of Triton X-100 (0.08% or 0.05%), the DRMs were able to hold the IRs, although in the TNFα-treated cells the IRs tended to shift to higher-density fractions.

Next, using membranes extracted with the 0.08% Triton X-100 buffer, we analyzed the distribution of GM3 and cholesterol and of proteins normally associated with DRMs (e.g., caveolin, flotillin, fyn), in each fraction of the sucrose density gradient (Figure 3). GM3 was preferentially localized at the DRMs in both normal and TNFα-treated 3T3-L1 adipocytes. Remarkably, though, the accumulation of GM3 observed in the DRMs was twofold higher in the TNFα-treated cells (Figure 3A). There were no distinct differences in the expression levels or distribution of cholesterol (Figure 3B), caveolin, flotillin, or fyn (Figure 3C). Taken together, these results clearly demonstrate the selective elimination of IRs from the DRMs and the

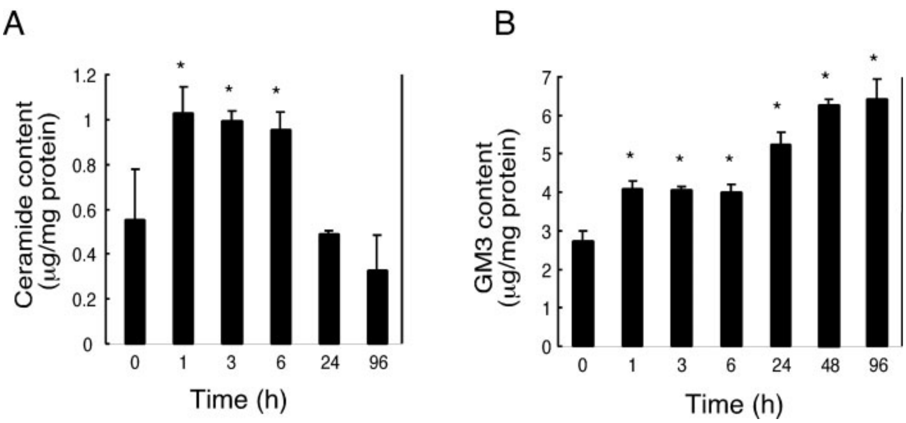

Fig. 1. GM3, but not ceramide, increases in adipocytes in a chronic state of insulin resistance. After treatment with 100 pM TNFα for various times (0–96 h), 3T3-L1 adipocytes were scraped, and total lipids were extracted. (**A**) Lipid samples were assayed for ceramide content using a DGK assay system as described under *Materials and methods*. (**B**) Ganglioside fractions were prepared from the extracted lipids and separated by TLC. GM3 content was quantified as described under *Materials and methods*. Data shown are means ± SD ($n = 3$). $*p < 0.05$.

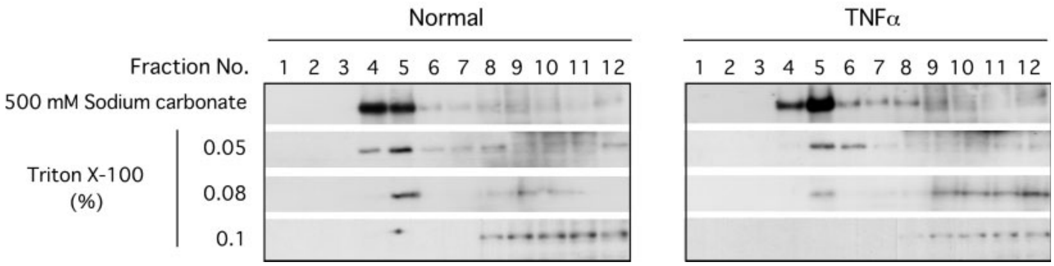

Fig. 2. IR can localize to DRMs in normal adipocytes but tends to shift to high-density fractions on TNFα treatment. TNFα-treated (96 h) or untreated adipocytes were homogenized with 500 mM sodium carbonate nondetergent buffer, or lysed with buffer containing detergent (0.05%, 0.08%, or 0.1% Triton X-100). Samples were then subjected to a sucrose density gradient flotation assay as described under *Materials and methods*. The gradient fractions from low (1) to high (12) density were subjected to SDS–PAGE and immunoblotted with an anti-IRβ antibody. This figure is a representative of three independent experiments.

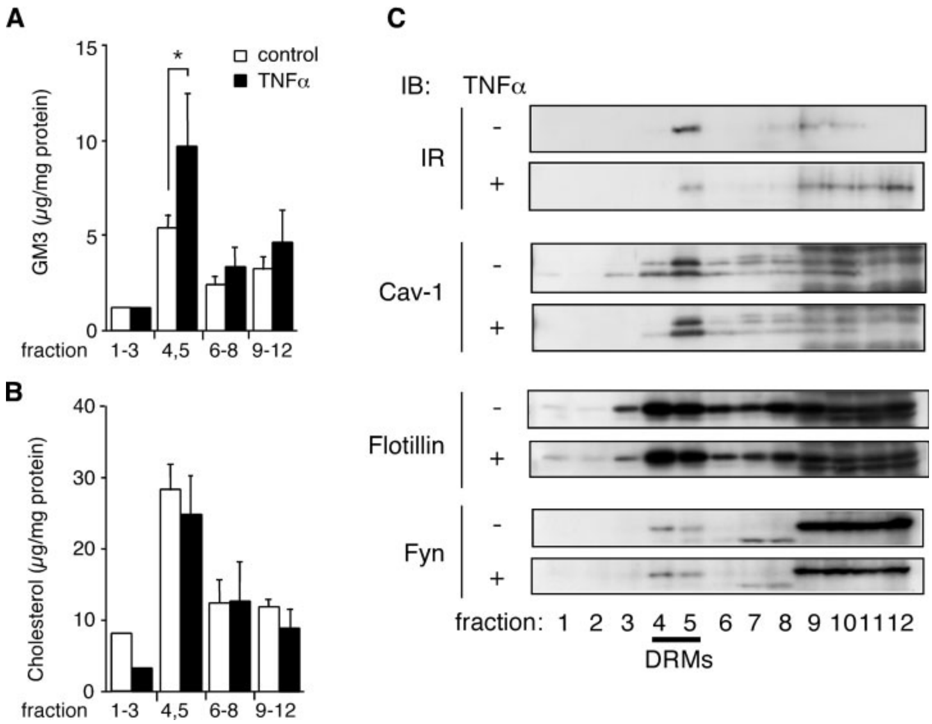

Fig. 3. Accumulation of GM3 in the DRMs and selective dissociation of IRs from DRMs in a state of insulin resistance. Adipocytes, untreated (open bars) or treated with 100 pM TNFα for 96 h (solid bars), were lysed with buffer containing 0.08% Triton X-100 and subjected to a sucrose density gradient floatation assay. (**A**) GM3 levels in the sucrose gradient fractions were examined by high-performance TLC analysis. (**B**) Cholesterol levels in the sucrose gradient fractions were measured by a commercial assay. (**C**) The samples were subjected to SDS–PAGE and immunoblotted with antibodies against IRβ, caveolin-1, flotillin, or fyn. Data in (**A**) and (**B**) are shown as means ± SD ($n = 3$). $*p < 0.05$. (**C**) is a representative of three independent experiments.

accumulation of GM3 in adipocytes under a chronic state of TNFα-induced insulin resistance.

TNFα selectively attenuates insulin-dependent IRS-1 tyrosine phosphorylation without affecting MAP kinase activation

Insulin signaling can be classified into mitogenic and metabolic activities. Mitogenic signaling was found to be normal in cells with impaired insulin-dependent internalization (Maggi *et al*., 1998; Parpal *et al*., 2001). Additionally, the prolonged treatment (at least 72 h) of 3T3-L1 adipocytes with low concentrations of TNFα (<0.1 nM) reportedly resulted in a pronounced inhibition of tyrosine phosphorylation of IRS-1 with little effect on IR autophosphorylation (Guo and Donner, 1996). We obtained similar results (Tagami *et al*., 2002). Under these conditions, we examined insulin-dependent mitogen-activated protein (MAP) kinase activation in TNFα-treated 3T3-L1 cells but found no suppression (Figure 4B), despite the selective inhibition of the insulin-dependent tyrosine phosphorylation of IRS-1 in these cells (Figure 4A).

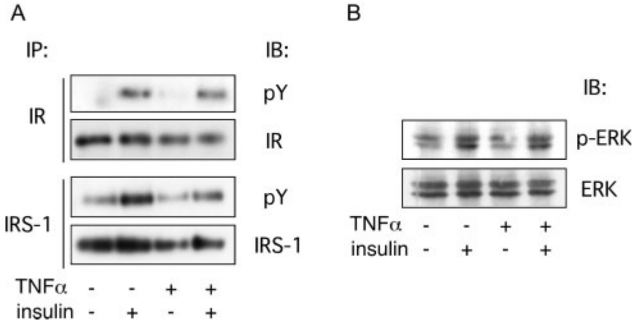

Fig. 4. TNFα selectively attenuates insulin-dependent IRS-1 tyrosine phosphorylation without affecting MAP kinase activation. 3T3-L1 adipocytes were cultured for 96 h in maintenance medium without or with 100 pM TNFα, then incubated for 6 h in serum-free medium containing 0.5% BSA in the absence or presence of TNFα. Cells were then stimulated with 100 nM insulin for 5 min. (**A**) Proteins in cell lysates were immunoprecipitated with an antiserum to IR or IRS-1, subjected to SDS–PAGE, and transferred to PVDF membrane. Western blotting was then performed with anti-phosphotyrosine (pY), anti-IRβ, or anti-IRS-1 antibodies. (**B**) For detection of insulin-dependent MAP kinase activation, the proteins in the cell lysates were subjected to SDS–PAGE and immunoblotted with anti-ERK and anti-phospho-ERK antibodies.

TNFα inhibits insulin-dependent IR internalization

The internalization of IR into endosomes and the subsequent intracellular movement of IRS-1 to the endosomes appear to be important steps in the metabolic signaling of insulin in adipocytes (Clark *et al.*, 2000; Klein *et al.*, 1987; Kublaoui *et al.*, 1995; Parpal *et al.*, 2001). Therefore, we examined the subcellular localization of IR, IRS-1, and GM3 in 3T3-L1 adipocytes, untreated or treated with insulin and/or TNFα (Figure 5). Cell fractions were obtained as illustrated in Figure 5A. Insulin-dependent IR internalization from P1 to P2 (Figure 5B, lanes 1 and 2) and insulin-dependent colocalization of IR (Figure 5B, lane 2) and IRS-1 (Figure 5C, lane 2) at P2 were evident. This movement allows the formation of an intracellular signaling complex that appears to be important for the metabolic signaling of insulin (glucose uptake). Under steady-state conditions, the major concentrations of IR and IRS-1 were localized at P1 and P3, respectively (Figure 5B, lane 1 versus Figure 5C, lane 1), but small amounts of IR and IRS-1 were colocalized in the P2 fraction, suggesting basal insulin signaling. However, TNFα treatment interfered with this colocalization (Figure 5B, lane 3 versus Figure 5C, lane 3). Furthermore, TNFα treatment resulted in the marked inhibition of insulin-dependent IR internalization (Figure 5B, lane 4) and translocation of IRS-1 from P3 to P2 and cytosol (Figure 5C, lane 4). Such suppression during TNFα-induced insulin resistance would essentially result in the inhibition of efficient intracellular signalosome formation.

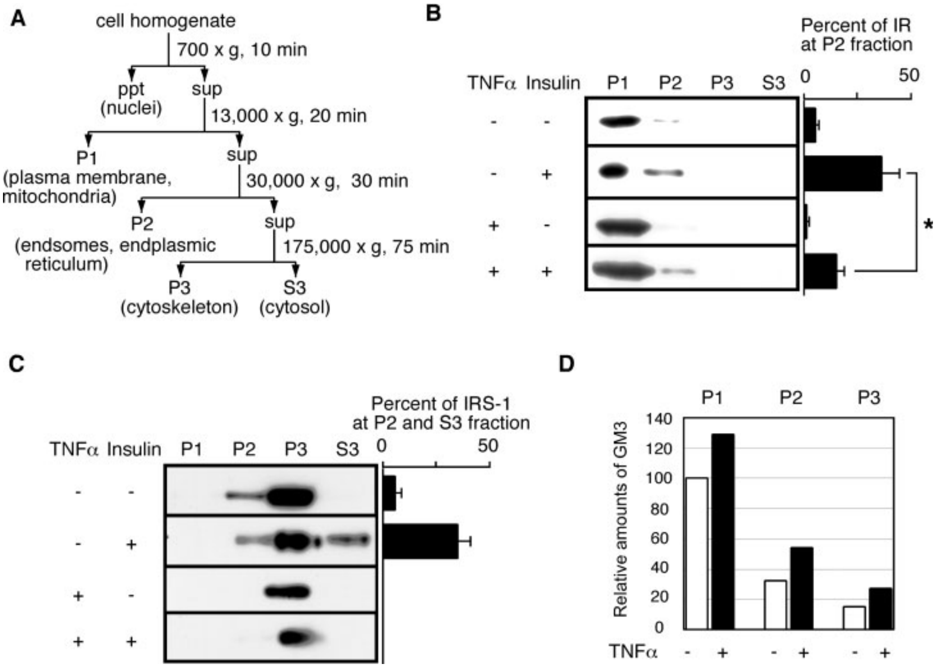

Fig. 5. TNFα inhibits insulin-dependent IR endocytosis. (**A**) Method of fractionation. 3T3-L1 adipocytes were cultured for 96 h in maintenance medium without or with TNFα, then incubated for 6 h in serum-free medium, containing 0.5% BSA, in the absence or presence of TNFα. Cells were stimulated with 100 nM insulin for 15 min. Homogenized cells were subjected to differential centrifugation to yield fractions enriched in plasma membranes (P1) and high-density microsomes (P2), then a high-speed pellet (P3) and a cytosol (S3) fraction. (**B** and **C**) Cell fractions (20 μg protein) were resolved by SDS–PAGE and immunoblotted with an anti-IRβ (**B**) or anti-IRS-1 (**C**) antibody. (**D**) Relative amounts of GM3 in the fractions of TNFα-treated or untreated adipocytes were determined as described under *Materials and methods*. Data in (**B**) and (**C**) are shown as means ± SD ($n = 3$). $*p < 0.05$.

To examine the subcellular distribution of GM3, we also analyzed the GM3 levels in the P1, P2, and P3 fractions of the adipocytes treated with or without TNFα. We found that GM3 was distributed throughout every fraction. Additionally, TNFα treatment increased GM3 levels almost equally in each fraction (Figure 5D).

GSL depletion attenuates the TNFα-induced inhibition of both insulin-stimulated IR internalization and elimination of IR from DRMs

To investigate whether the inhibition of insulin-dependent IR internalization and the elimination of IR from the microdomains in TNFα-treated cells were due to increases in GM3, we employed an inhibitor of glucosylceramide synthase, D-*threo*-1-phenyl-2-decanoylamino-3-morpholino-1-propanol (D-PDMP). After GM3 depletion by D-PDMP, the suppression of IR internalization was indeed partially recovered (Figure 6A). Additionally, the elimination of IRs from the DRMs was effectively blocked (Figure 6B). There was no obvious change in the accumulation of IR in the DRMs after insulin stimulation (data not shown). That D-PDMP treatment was able to counteract the TNFα-induced inhibition of both insulin-stimulated IR internalization and elimination of IRs from the DRMs indicates direct involvement of GM3 in the chronic state of insulin resistance in adipocytes.

Discussion

Caveolae are a subset of membrane microdomains particularly abundant in adipocytes (Fan *et al.*, 1983). Critical dependence of the insulin metabolic signal transduction on caveolae/microdomains in adipocytes has been demonstrated. Disruption of microdomains by cholesterol extraction with β-cyclodextrin resulted in progressive inhibition of tyrosine phosphorylation of IRS-1 and activation of glucose transport in response to insulin although autophosphorylation of IR and activation of MAP kinase were not impaired (Parpal *et al.*, 2001). Similarities between these cell culture results and the findings in many cases of clinical insulin resistance (Virkamaki *et al.*, 1999), thereby suggesting a potential role for microdomains in the pathogenesis of this disorder. Gangliosides are also known as structurally and functionally important components in microdomains, however, there has been no report on their role(s) in microdomains in adipocytes.

In a previous study of insulin resistance induced in adipocytes by TNFα, we presented evidence that the transformation to a resistant state may depend on increased ganglioside GM3 biosynthesis following up-regulated SAT-1 gene expression. Additionally, GM3 may function as an inhibitor of insulin signaling during chronic exposure to TNFα (Tagami *et al.*, 2002). These findings are further supported by the recent report that mice lacking SAT-1 exhibit enhanced insulin signaling (Yamashita *et al.*, 2003). Because GSLs, including GM3, are important components of DRMs/caveolae, we pursued the possibility that increased GM3 levels in DRMs confer insulin resistance on TNFα-treated 3T3-L1 adipocytes.

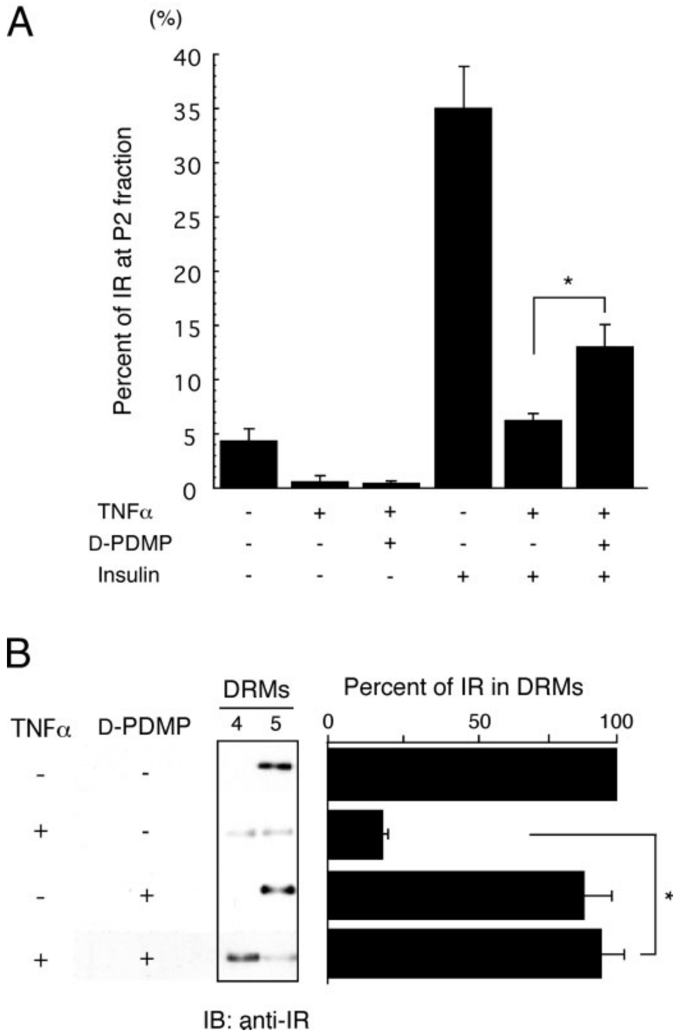

Fig. 6. GM3 depletion attenuates TNFα-induced inhibition of both insulin-stimulated IR internalization and elimination of IR from the DRMs. (**A**) 3T3-L1 adipocytes were cultured in maintenance medium with or without TNFα for 96 h in the presence or absence of 20 μM D-PDMP. Cells were further incubated for 8 h in serum-free medium containing 0.5% BSA in the absence or presence of TNFα and D-PDMP as descirbed, then stimulated with 100 nM insulin for 15 min. The cells were subjected to differential centrifugation as in Figure 2, and the fractions were assayed by SDS–PAGE and immunoblotting with an anti-IRβ antibody. (**B**) 3T3-L1 cells were cultured in maintenance medium with or without TNFα for 96 h in the presence or absence of 20 μM D-PDMP. The cells were lysed with buffer containing 0.08% Triton X-100, and the lysates were subjected to a sucrose density gradient floatation assay as described under *Materials and methods*. The gradient fractions, from low (1) to high (12) density, were subjected to SDS–PAGE and immunoblotted with an anti-IRβ antibody. Data shown are means ± SD ($n = 3$). $^{*}p < 0.05$.

Evidence suggesting that caveolae and caveolins play a major role in insulin signaling initially came from experiments using rat adipocytes, in which gold-labeled insulin was endocytosed by a mechanism involving clathrin-independent, uncoated invaginations (Goldberg *et al.*, 1987). Immunogold electron (Gustavsson *et al.*, 1999) and immunofluorescence microscopy (Kimura *et al.*, 2002) further demonstrated that IRs are highly concentrated in caveolae. Additionally, Couet *et al.* (1997) demonstrated the presence of a caveolin binding motif (ϕXXXX ϕXXϕ) in the β subunit of IRs that could bind to the scaffold domain of caveolin. Moreover, mutation of this motif resulted in the inhibition of insulin signaling (Nystrom *et al.*, 1999). Indeed, mutations of the IRβ subunit have been found in type 2 diabetes patients (Imamura *et al.*, 1994, 1998; Iwanishi *et al.*, 1993). Recently, Lisanti's laboratory reported that caveolin-1-null mice developed insulin resistance when placed on a high-fat diet (Cohen *et al.*, 2003a). Interestingly, insulin signaling, as measured by IR phosphorylation and its downstream targets, was selectively decreased in the adipocytes of these animals while signaling in both muscle and liver cells was normal (Cohen *et al.*, 2003a). This signaling defect was attributed to a 90% decrease in IR protein content in the adipocytes, with no changes in mRNA levels, indicating that caveolin-1 serves to stabilize the IR protein (Cohen *et al.*, 2003a,b). These studies clearly indicate the critical importance of the interaction between caveolin and IR in executing successful insulin signaling in adipocytes.

Saltiel and colleagues (Mastick *et al.*, 1995) found that insulin stimulation of 3T3-L1 adipocytes was associated with tyrosine phosphorylation of caveolin-1. However, because only trace levels of IR were recovered in the caveolae microdomains in assays with a buffer of 1% Triton X-100, they speculated on the presence of intermediate molecule(s) bridging IR and caveolin (Mastick and Saltiel, 1997). Gustavsson *et al.* (1999) also observed the dissociation of IRs from caveolin-containing DRMs after treatments of 0.3 and 0.1% Triton X-100. It has been reported that comparison of protein and lipid contents of DRMs prepared with a variety of detergents exhibited the considerable differences in their ability to selectively solubilize membrane proteins and to enrich sphingolipids and cholesterol over glycerophospholipids, and Triton was the most reliable detergent (Schuck *et al.*, 2003). Therefore we performed a flotation assay with a wide range of Triton X-100 concentrations to identify the protein of interest that might weakly associate with DRMs.

In an assay system containing less than 0.08% Triton X-100, we were able to show that in normal adipocyte IRs can localize to DRMs., However, in the presence of TNFα, IR was selectively eliminated from the DRMs, whereas caveolin-1 remained (Figure 3C). Thus by employing low detergent concentrations we were able to demonstrate for the first time the presence of IR in DRMs. We currently believe that elimination of IR from the DRMs by TNFα treatment is due to an excessive accumulation of GM3 in these microdomains, especially because preventing GM3 biosynthesis using D-PDMP attenuated the elimination of IR from the DRMs (Figure 6B). Reportedly, the localization in the DRMs of several proteins (including receptor protein tyrosine kinases) can be affected by changes in the expression levels of GSLs. For example, overexpression of the ganglioside GM1 in Swiss 3T3 cells results in the dispersion of β type platelet-derived growth factor receptor from the DRMs (Mitsuda *et al.*, 2002). Similarly, the genetically enhanced accumulation of endogenous GM3 in keratinocytes caused the dissociation of caveolin-1 from the DRMs, thereby changing the signaling of the epidermal growth factor receptor (Wang *et al.*, 2002). In HuH7 hepatoma cells, which lack caveolin, IRs associate with DRMs in response to insulin stimulation, but cross-linking of GM2 by its antibody results in a loss of this association (Vainio *et al.*, 2002). Such results support the likelihood that localization of IRs to the DRMs is affected by the presence of not only caveolin but also GSLs, especially gangliosides.

Studies in adipocytes have implicated the endosomal apparatus as the site of insulin-stimulated IRS-1 tyrosine phosphorylation by activated IR kinase and associated PI-3 kinase activation (Kublaoui *et al.*, 1995). Likewise, in isolated adipocytes treated with insulin, tyrosine-phosphorylated IRS-1 levels and PI-3 kinase activity were 10-fold greater in microsomes than at the plasma membrane (Kelly and Ruderman, 1993). The time course for the accumulation of internalized IR kinase closely paralleled the time course of the IRS-1 phosphorylation (Kublaoui *et al.*, 1995). Additionally, the C860S mutation in the extracellular domain of the β subunit of IR was found to reduce insulin-stimulated IR internalization, as well as IRS-1 tyrosine phosphorylation, without changing the autophosphorylation of IR and MAP kinase activation (Maggi *et al.*, 1998). Collectively, all these data strongly suggest that the autophosphorylation of IR in response to insulin stimulation will not be affected by the IR localization in membranes such as caveolin-rich microdomains (raft) or nonraft membranes in adipocytes but the successful internalization of the IR through microdomains is necessary for tyrosine phosphorylation of IRS-1.

There have been no reports on IR internalization in a state of insulin resistance induced by TNFα. We found that in TNFα-treated 3T3-L1 adipocytes the insulin-dependent IR internalization and the intracellular movement of IRS-1 were greatly suppressed, leading to an uncoupling of the IR–IRS-1 signaling (Figure 5). Additionally, tyrosine phosphorylation of IRS-1 in response to insulin was selectively impaired without affecting the activation of IR and MAP kinase (Figure 4). The observed impairment of IR internalization by TNFα may be attributed to the elimination of IR from microdomains due to the excess accumulation of GM3 (Figures 3A and 3C). Although the localization of IRs to DRMs may be maintained by the association with caveolin-1 as mentioned, the excess accumulation of GM3 in the DRMs may weaken IR-caveolin interaction. Indeed, IR but not caveolin-1 was coimmunoprecipitated with anti-GM3 antibody (unpublished data). Further work is needed to elucidate the mechanisms for the interactions of the ganglioside GM3, IR, and caveolin in the microdomains.

The reason for the complete interruption of the IRS-1 movement in the TNFα-treated adipocytes on insulin stimulation is worthy of further studies, including those into the role of intracellular GM3 (Figure 5D). Indeed, GSLs are also known to be internalized via a clathrin-independent mechanism (Marks and Pagano, 2002; Puri *et al.*, 2001). We are in the process of expanding our studies regarding the functional and structural changes of microdomains in the state of insulin resistance and type 2 diabetes.

We employed an inhibitor of glucosylceramide synthase, D-PDMP (Inokuchi and Radin, 1987; Radin *et al.*, 1993), to deplete cellular GSLs derived from glucosylceramide. This inhibitor is able to reduce the ganglioside content with minimum effect on phospholipids, neutral lipids, and glycoproteins (Barbour *et al.*, 1992). D-PDMP was able to counteract the TNFα-induced increase in GM3 content in adipocytes and to normalize the TNFα-induced defect in the tyrosine phosphorylation of IRS-1 in response to insulin stimulation, as reported previously (Tagami *et al.*, 2002). Moreover, this inhibitor was able to counteract the TNFα-induced suppression of IR internalization (Figure 6A) and IR elimination from DRMs (Figure 6B) required for insulin metabolic signaling, inspiring a new therapeutic strategy we have termed microdomain ortho-signaling therapy. Thus we were encouraged to measure the effect of D-PDMP on the TNFα-induced defect of glucose uptake, but so far have not observed any recovery (data not shown). Nevertheless, the possible therapeutic implication for insulin resistance will be pursued more extensively. Toward this end, we have recently succeeded in developing a new potent inhibitor of glucosyl ceramide synthase (D-PDMP) and its analogs, which have no general cytotoxic effect (Jimbo *et al.*, 2000).

Materials and methods

Cell line and culture conditions

Murine 3T3-L1 preadipocytes were cultured, maintained, and differentiated as described previously (Tagami *et al.*, 2002). Recombinant human TNFα (Genzyme-Techne, Cambridge, MA) was dissolved in phosphate-buffered saline (PBS) containing 0.1% fatty acid–free, growth factor–depleted bovine serum albumin (BSA; Sigma-Aldrich, Japan) and then added directly to the cell culture media at a concentration of 100 pM. After culturing for 96 h, the media on the treated cells and untreated controls were replaced with serum-free Dulbecco's modified Eagle medium containing 0.5% BSA, with or without 100 pM TNFα, for 6 h. For insulin studies, the cells were stimulated with 100 nM insulin for 5 or 15 min as specified. Cellular GSLs were depleted using 20 μM D-PDMP, an inhibitor of glucosylceramide synthase, synthesized as described previously (Inokuchi and Radin, 1987).

Immunoprecipitation and immunoblotting

Cell extracts from adipocytes were prepared as described previously (Tagami *et al.*, 2002). IR and IRS-1 were immunopurified with specific antibodies preadsorbed to protein A/G-Sepharose (Santa Cruz Biotechnology, Santa Cruz, CA) then submitted to sodium dodecyl sulfate (SDS)–polyacrylamide gel electrophoresis (PAGE) under reducing conditions (Tagami *et al.*, 2002). Anti-Fyn (FYN3) and anti-phospho-ERK (E-4) antibodies and peroxidase-conjugated anti-rabbit IgG and peroxidase-conjugated anti-mouse IgG were from the same supplier. Western blot analysis was performed using the ECL western blot kit (Amersham Biosciences, Buckinghamshire, UK) and the Lumi-Light Plus western blotting substrate (Roche, Mannheim, Germany). Anti-p44/42 MAP kinase (ERK) rabbit polyclonal antibody was purchased from Cell Signaling (Beverly, MA). Anti-IRS-1 rabbit antiserum was from Upstate Biotechnology (Lake Placid, NY). Anti-caveolin-1, anti-flotillin-1, and anti-phosphotyrosine monoclonal PY20 antibodies were all purchased from BD Transduction Laboratories (Lexington, KY). For use in protein determination assays, bicinchoninic acid reagent was obtained from Pierce Chemical (Rockford, IL).

Lipid and cholesterol analyses

Total lipids were extracted from cells with chloroform:-methanol (1:1 and 1:2, v/v, successively), and purified as described elsewhere (Inokuchi *et al.*, 1989) to obtain the acidic glycolipid fraction. GM3, the primary ganglioside in these cells (Reed *et al.*, 1980), was quantified with a dual-wavelength flying spot scanner (CS9000; Shimadzu, Kyoto, Japan) at a reflectance mode of 500 nm, with area integration. Standard GM3 was kindly provided by Snow Brand Foods (Saitama, Japan). Cholesterol levels were determined using the Cholesterol CII assay kit (Wako, Osaka, Japan). Ceramide levels in total lipid extracts of 3T3-L1 cells were measured using a modified version of the diacylglycerol kinase (DGK) assay of Preiss *et al.* (1986) Briefly, 20 μl micellar lipids were added to 0.2 μl dithiothreitol (1 M), 2 μl *Escherichia coli* DGK (7.1 U/ml), 1 μl [γ-^{32}P]ATP (10 mCi/ml in tricine buffer, pH 6.7), 50 μl reaction buffer (100 mM imidazole, pH 6.6, 100 mM LiCl, 25 mM $MgCl_2$, and 2 mM ethylene glycol bis(2-aminoethyl ether)-tetra acetic acid, pH 6.6), and 17.8 μl dilution buffer (100 mM imidazole, pH 6.6, with 1 mM diethylenetriamine penta-acetic acid). After incubating for 30 min at 37°C, lipids were extracted with 0.6 ml chloroform:methanol (1:1, v/v). After vortexing, 265 μl of 1 M KCl was added, and the phases were separated by centrifugation. An aliquot of the organic phase was dried, resuspended with 20 μl chloroform, and spotted on a high-performance thin-layer chromatography plate. Lipids were separated in chloroform:acetone:methanol:acetic acid:water (10:4:3:2:1). Radioactive bands were visualized with an imaging analyzer (BAS-2000, Fuji Film), and ^{32}P-ceramide-1-phosphate was quantified.

Cell fractionation

IRs and IRS-1s were fractionated from 3T3-L1 adipocytes as described previously (Clark *et al.*, 2000) with slight modifications as illustrated in Figure 2. All procedures were performed at 4°C. Briefly, cell homogenates were centrifuged at $700 \times g$ for 10 min to remove nuclei and large cellular debris. The supernatant was centrifuged at $13{,}000 \times g$ for 20 min to pellet the plasma membrane and mitochondria. This supernatant was subjected to further centrifugation at $30{,}000 \times g$ for 30 min to pellet the high-density microsomal fraction. The resultant supernatant was subjected to a final centrifugation at $175{,}000 \times g$ for 75 min to obtain the high-speed pellet, and the supernatant from this centrifugation was designated the cytosol fraction. The high-speed pellet was solubilized in 1% SDS in PBS.

Sucrose gradient centrifugation

All steps were carried out at 4°C. Differentiated 3T3-L1 adipocytes were washed with PBS and lysed in 2 ml TNE buffer (10 mM Tris–HCl, pH 7.5, 150 mM NaCl, 5 mM ethylenediamine tetra-acetic acid), containing protease inhibitors and 2 mM Na_3VO_4 and various concentrations of Triton X-100. Lysates were centrifuged for 5 min at $1300 \times g$ to remove nuclei and large cellular debris, and the supernatants were diluted with equal volumes of 85% (w/v) sucrose in TNE buffer. In an ultracentrifuge tube the diluted lysates were overlaid with 4 ml 30% sucrose (w/v) in TNE buffer, then with 4 ml 5% sucrose (w/v) in TNE buffer. The samples were centrifuged at 39,000 rpm for 18 h in an SW41 rotor (Beckman Instruments, Palo Alto, CA), and 1-ml fractions were collected from the top for immunoblotting and lipid analysis.

For the nondetergent sucrose density gradient, 3T3-L1 adipocytes were washed with PBS and rapidly scraped into 2 ml 500 mM sodium carbonate buffer (pH 11), then homogenized using a Polytron tissue grinder (three 10-s bursts; Kinematica GmbH, Brinkmann Instruments, Westbury, NY). The homogenates were then sonicated three times for 20 s. All homogenates were centrifuged for 5 min at $1300 \times g$ to remove nuclei and large cellular debris. Each homogenate was then adjusted to 42.5% sucrose by the addition of 2 ml 85% sucrose prepared in MBS (25 mM 2-(*N*-morpholino)ethanesulfonic acid, pH 6.5, with 150 mM NaCl). The solution (4 ml) was placed at the bottom of an ultracentrifuge tube. Above this, a 5–35% discontinuous sucrose gradient was formed (4 ml 5% sucrose/4 ml 35% sucrose, both in MBS containing 250 mM sodium carbonate). The tube was centrifuged at 39,000 rpm for 18 h in an SW41 rotor and the total solutions was fractionated as already described.

Acknowledgments

We thank Dr. Norman S. Radin (University of Michigan) for valuable comments. This study was supported in part by grants-in aid 15390019 (to J.I.) and 15040202 (Scientific Research on Priority Area to J.I.) from the Ministry of Education, Culture, Sports, Science and Technology. This work was also supported by the Mizutani Foundation for Glycoscience (to J.I.).

Abbreviations

BSA, bovine serum albumin; DGK, diacylglycerol kinase; D-PDMP, D-*threo*-1-phenyl-2-decanoylamino-3-morpholino-1-propanol; DRM, detergent-resistant membrane microdomain; GSL, glycosphingolipid; IR, insulin receptor; IRS-1, insulin receptor substrate-1; MAP, mitogen-activated protein; PAGE, polyacrylamide gel electrophoresis; PBS, phosphate-buffered saline; SAT-I, GM3 synthase; SDS, sodium dodecyl sulfate; TNFα, tumor necrosis factor alpha.

References

Barbour, S., Edidin, M., Felding-Habermann, B., Taylor-Norton, J., Radin, N.S., and Fenderson, B.A. (1992) Glycolipid depletion using a ceramide analogue (PDMP) alters growth, adhesion, and membrane lipid organization in human A431 cells. *J. Cell Physiol.*, **150**, 610–619.

Bickel, P.E. (2002) Lipid rafts and insulin signaling. *Am. J. Physiol. Endocrinol. Metab.*, **282**, E1–E10.

Brindley, D.N., Wang, C.N., Mei, J., Xu, J., and Hanna, A.N. (1999) Tumor necrosis factor-alpha and ceramides in insulin resistance. *Lipids*, **34**, S85–S88.

Clark, S.F., Molero, J.C., and James, D.E. (2000) Release of insulin receptor substrate proteins from an intracellular complex coincides with the development of insulin resistance. *J. Biol. Chem.*, **275**, 3819–3826.

Cohen, A.W., Razani, B., Wang, X.B., Combs, T.P., Williams, T.M., Scherer, P.E. and Lisanti, M.P. (2003a) Caveolin-1-deficient mice show insulin resistance and defective insulin receptor protein expression in adipose tissue. *Am. J. Physiol. Cell Physiol.*, **285**, C222–C235.

Cohen, A.W., Combs, T.P., Scherer, P.E., and Lisanti, M.P. (2003b) Role of caveolin and caveolae in insulin signaling and diabetes. *Am. J. Physiol. Endocrinol. Metab.*, **285**, E1151–E1160.

Couet, J., Li, S., Okamoto, T., Ikezu, T., and Lisanti, M.P. (1997) Identification of peptide and protein ligands for the caveolin-scaffolding domain. Implications for the interaction of caveolin with caveolae-associated proteins. *J. Biol. Chem.*, **272**, 6525–6533.

Fan, J.Y., Carpentier, J.L., van Obberghen, E., Grunfeld, C., Gorden, P., and Orci, L. (1983) Morphological changes of the 3T3-L1 fibroblast plasma membrane upon differentiation to the adipocyte form. *J. Cell Sci.*, **61**, 219–230.

Goldberg, R.I., Smith, R.M., and Jarett, L. (1987) Insulin and alpha 2-macroglobulin-methylamine undergo endocytosis by different mechanisms in rat adipocytes: I. Comparison of cell surface events. *J. Cell Physiol.*, **133**, 203–212.

Guo, D. and Donner, D.B. (1996) Tumor necrosis factor promotes phosphorylation and binding of insulin receptor substrate 1 to phosphatidylinositol 3-kinase in 3T3-L1 adipocytes. *J. Biol. Chem.*, **271**, 615–618.

Gustavsson, J., Parpal, S., Karlsson, M., Ramsing, C., Thorn, H., Borg, M., Lindroth, M., Peterson, K.H., Magnusson, K.E., and Stralfors, P. (1999) Localization of the insulin receptor in caveolae of adipocyte plasma membrane. *FASEB J.*, **13**, 1961–1971.

Hakomori, S.I. (2000) Cell adhesion/recognition and signal transduction through glycosphingolipid microdomain. *Glycoconj. J.*, **17**, 143–151.

Hannun, Y.A. (1994) The sphingomyelin cycle and the second messenger function of ceramide. *J. Biol. Chem.*, **269**, 3125–3128.

Hotamisligil, G.S., Shargill, N.S. and Spiegelman, B.M. (1993) Adipose expression of tumor necrosis factor-alpha: direct role in obesity-linked insulin resistance. *Science*, **259**, 87–91.

Hotamisligil, G.S., Arner, P., Caro, J.F., Atkinson, R.L. and Spiegelman, B.M. (1995) Increased adipose tissue expression of tumor necrosis factor-alpha in human obesity and insulin resistance. *J. Clin. Invest.*, **95**, 2409–2415.

Imamura, T., Takata, Y., Sasaoka, T., Takada, Y., Morioka, H., Haruta, T., Sawa, T., Iwanishi, M., Hu, Y.G., Suzuki, Y. and others. (1994) Two naturally occurring mutations in the kinase domain of insulin receptor accelerate degradation of the insulin receptor and impair the kinase activity. *J. Biol. Chem.*, **269**, 31019–31027.

Imamura, T., Haruta, T., Takata, Y., Usui, I., Iwata, M., Ishihara, H., Ishiki, M., Ishibashi, O., Ueno, E., Sasaoka, T., and Kobayashi, M. (1998) Involvement of heat shock protein 90 in the degradation of mutant insulin receptors by the proteasome. *J. Biol. Chem.*, **273**, 11183–11188.

Inokuchi, J. and Radin, N. (1987) Preparation of the active isomer of 1-phenyl-2-decanoylamino-3-morpholino-1-propanol, inhibitor of murine glucocerebroside synthetase. *J. Lipid Res.*, **28**, 565–571.

Inokuchi, J., Momosaki, K., Shimeno, H., Nagamatsu, A., and Radin, N.S. (1989) Effects of D-threo-PDMP, an inhibitor of glucosylceramide synthetase, on expression of cell surface glycolipid antigen and binding to adhesive proteins by B16 melanoma cells. *J. Cell Physiol.*, **141**, 573–583.

Iwanishi, M., Haruta, T., Takata, Y., Ishibashi, O., Sasaoka, T., Egawa, K., Imamura, T., Naitou, K., Itazu, T. and Kobayashi, M. (1993) A mutation (Trp1193 → Leu1193) in the tyrosine kinase domain of the insulin receptor associated with type A syndrome of insulin resistance. *Diabetologia*, **36**, 414–422.

Jimbo, M., Yamagishi, K., Yamaki, T., Nunomura, K., Kabayama, K., Igarashi, Y., and Inokuchi, J.I. (2000) Development of a new inhibitor of glucosylceramide synthase. *J. Biochem. (Tokyo)*, **127**, 485–491.

Kanety, H., Hemi, R., Papa, M.Z., and Karasik, A. (1996) Sphingomyelinase and ceramide suppress insulin-induced tyrosine phosphorylation of the insulin receptor substrate-1. *J. Biol. Chem.*, **271**, 9895–9897.

Kelly, K.L. and Ruderman, N.B. (1993) Insulin-stimulated phosphatidylinositol 3-kinase. Association with a 185-kDa tyrosine-phosphorylated protein (IRS-1) and localization in a low density membrane vesicle. *J. Biol. Chem.*, **268**, 4391–4398.

Kimura, A., Mora, S., Shigematsu, S., Pessin, J.E. and Saltiel, A.R. (2002) The insulin receptor catalyzes the tyrosine phosphorylation of caveolin-1. *J. Biol. Chem.*, **277**, 30153–30158.

Klein, H.H., Freidenberg, G.R., Matthaei, S., and Olefsky, J.M. (1987) Insulin receptor kinase following internalization in isolated rat adipocytes. *J. Biol. Chem.*, **262**, 10557–10564.

Kublaoui, B., Lee, J., and Pilch, P.F. (1995) Dynamics of signaling during insulin-stimulated endocytosis of its receptor in adipocytes. *J. Biol. Chem.*, **270**, 59–65.

Maggi, D., Andraghetti, G., Carpentier, J.L., and Cordera, R. (1998) Cys860 in the extracellular domain of insulin receptor beta-subunit is critical for internalization and signal transduction. *Endocrinology*, **139**, 496–504.

Marks, D.L. and Pagano, R.E. (2002) Endocytosis and sorting of glycosphingolipids in sphingolipid storage disease. *Trends Cell Biol.*, **12**, 605–613.

Mastick, C.C. and Saltiel, A.R. (1997) Insulin-stimulated tyrosine phosphorylation of caveolin is specific for the differentiated adipocyte phenotype in 3T3-L1 cells. *J. Biol. Chem.*, **272**, 20706–20714.

Mastick, C.C., Brady, M.J., and Saltiel, A.R. (1995) Insulin stimulates the tyrosine phosphorylation of caveolin. *J. Cell Biol.*, **129**, 1523–1531.

Mitsuda, T., Furukawa, K., Fukumoto, S., Miyazaki, H., and Urano, T. (2002) Overexpression of ganglioside GM1 results in the dispersion of platelet-derived growth factor receptor from glycolipid-enriched microdomains and in the suppression of cell growth signals. *J. Biol. Chem.*, **277**, 11239–11246.

Muller, G., Jung, C., Wied, S., Welte, S., Jordan, H., and Frick, W. (2001) Redistribution of glycolipid raft domain components induces insulin-mimetic signaling in rat adipocytes. *Mol. Cell Biol.*, **21**, 4553–4567.

Nystrom, F.H., Chen, H., Cong, L.N., Li, Y., and Quon, M.J. (1999) Caveolin-1 interacts with the insulin receptor and can differentially modulate insulin signaling in transfected COS-7 cells and rat adipose cells. *Mol. Endocrinol.*, **13**, 2013–2024.

Ohashi, M. (1979) A comparison of the ganglioside distributions of fat tissues in various animals by two-dimensional thin layer chromatography. *Lipids*, **14**, 52–57.

Parpal, S., Karlsson, M., Thorn, H., and Stralfors, P. (2001) Cholesterol depletion disrupts caveolae and insulin receptor signaling for metabolic control via insulin receptor substrate-1, but not for mitogen-activated protein kinase control. *J. Biol. Chem.*, **276**, 9670–9678.

Peraldi, P., Hotamisligil, G.S., Buurman, W.A., White, M.F., and Spiegelman, B.M. (1996) Tumor necrosis factor (TNF)-alpha inhibits insulin signaling through stimulation of the p55 TNF receptor and activation of sphingomyelinase. *J. Biol. Chem.*, **271**, 13018–13022.

Preiss, J., Loomis, C.R., Bishop, W.R., Stein, R., Niedel, J.E., and Bell, R.M. (1986) Quantitative measurement of sn-1,2-diacylglycerols present in platelets, hepatocytes, and ras- and sis-transformed normal rat kidney cells. *J Biol. Chem.*, **261**, 8597–8600.

Puri, V., Watanabe, R., Singh, R.D., Dominguez, M., Brown, J.C., Wheatley, C.L., Marks, D.L., and Pagano, R.E. (2001) Clathrin-dependent and -independent internalization of plasma membrane sphingolipids initiates two Golgi targeting pathways. *J. Cell Biol.*, **154**, 535–547.

Radin, N.S., Shayman, J.A., and Inokuchi, J. (1993) Metabolic effects of inhibiting glucosylceramide synthesis with PDMP and other substances. *Adv. Lipid Res.*, **26**, 183–213.

Reed, B.C., Moss, J., Fishman, P.H., and Lane, M.D. (1980) Loss of choleragen receptors and ganglioside upon differentiation of 3T3-L1 preadipocytes. *J. Biol. Chem.*, **255**, 1711–1715.

Schuck, S., Honsho, M., Ekroos, K., Shevchenko, A., and Simons, K. (2003) Resistance of cell membranes to different detergents. *Proc. Natl Acad. Sci. USA*, **100**, 5795–5800.

Simons, K. and Toomre, D. (2000) Lipid rafts and signal transduction. *Nat. Rev. Mol. Cell Biol.*, **1**, 31–39.

Tagami, S., Inokuchi Ji, J., Kabayama, K., Yoshimura, H., Kitamura, F., Uemura, S., Ogawa, C., Ishii, A., Saito, M., Ohtsuka, Y., and others. (2002) Ganglioside GM3 participates in the pathological conditions of insulin resistance. *J. Biol. Chem.*, **277**, 3085–3092.

Uysal, K.T., Wiesbrock, S.M., Marino, M.W., and Hotamisligil, G.S. (1997) Protection from obesity-induced insulin resistance in mice lacking TNF-alpha function. *Nature*, **389**, 610–614.

Vainio, S., Heino, S., Mansson, J.E., Fredman, P., Kuismanen, E., Vaarala, O. and Ikonen, E. (2002) Dynamic association of human insulin receptor with lipid rafts in cells lacking caveolae. *EMBO Rep.*, **3**, 95–100.

Virkamaki, A., Ueki, K., and Kahn, C.R. (1999) Protein-protein interaction in insulin signaling and the molecular mechanisms of insulin resistance. *J. Clin. Invest.*, **103**, 931–943.

Wang, X.Q., Sun, P., and Paller, A.S. (2002) Ganglioside induces caveolin-1 redistribution and interaction with the epidermal growth factor receptor. *J. Biol. Chem.*, **277**, 47028–47034.

Yamashita, T., Hashiramoto, A., Haluzik, M., Mizukami, H., Beck, S., Norton, A., Kono, M., Tsuji, S., Daniotti, J.L., Werth, N., and others. (2003) Enhanced insulin sensitivity in mice lacking ganglioside GM3. *Proc. Natl Acad. Sci. USA*, **100**, 3445–3449.